Germann J, Gouveia FV, Chakravarty MM, Devenyi GA. Longitudinal deformation-based morphometry pipeline to study neuroanatomical differences in structural MRI based on SyN unbiased templates. *Aperture Neuro*. 2025;5. doi:10.52294/001c.133510

Original Research Articles

Longitudinal deformation-based morphometry pipeline to study neuroanatomical differences in structural MRI based on SyN unbiased templates

Jurgen Germann, Ph.D.[1,2,3] [a], Flavia Venetucci Gouveia, Ph.D.[4], M. Mallar Chakravarty, Ph.D.[5,6], Gabriel A. Devenyi, Ph.D.[5,6] [b]

[1] Center for Advancing Neurotechnological Innovation to Application (CRANIA), [2] Division of Brain, Imaging and Behaviour, Krembil Research Institute, [3] Institute of Biomedical Engineering, University of Toronto, [4] Neuroscience and Mental Health, Hospital for Sick Children, [5] Department of Psychiatry, McGill University, [6] Cerebral Imaging Centre, Douglas Mental Health University Institute

Keywords: deformation-based morphometry, longitudinal morphometry, minimal deformation average, volumetric brain changes

https://doi.org/10.52294/001c.133510

Aperture Neuro

Vol. 5, 2025

Morphometric measures in humans derived from magnetic resonance imaging (MRI) have provided important insights into brain differences and changes associated with development and disease in vivo. Deformation-based morphometry (DBM) is a registration-based technique that has been shown to be useful in detecting local volume differences and longitudinal brain changes while not requiring a priori segmentation or tissue classification. Typically, DBM measures are derived from registration to common template brain space (one-level DBM). Here, we present a two-level DBM technique: first, the Jacobian determinants are calculated for each individual input MRI at the subject level to capture longitudinal individual brain changes; then, in a second step, an unbiased common group space is created, and the Jacobians co-registered to enable the comparison of individual morphological changes across subjects or groups. This two-level DBM is particularly suitable for capturing longitudinal intra-individual changes in vivo, as calculating the Jacobians within-subject space leads to superior accuracy. Using artificially induced volume differences, we demonstrate that this two-level DBM pipeline is 4.5x more sensitive in detecting longitudinal within-subject volume changes compared to a typical one-level DBM approach. It also captures the magnitude of the induced volume change much more accurately. Using 150 subjects from the OASIS-2 dataset, we demonstrate that the two-level DBM is superior in capturing cortical volume changes associated with cognitive decline across patients with dementia and cognitively healthy individuals. This pipeline provides researchers with a powerful tool to study longitudinal brain changes with superior accuracy and sensitivity. It is publicly available and has already been used successfully, proving its utility.

a Corresponding author:
Jürgen Germann
Krembil Brain Institute
University Health Network
399 Bathurst Street
Toronto, ON, Canada, M5T 2S8
germannj@gmail.com

b Corresponding author:
Gabriel A. Devenyi
Douglas Mental Health University Institute
Cerebral Imaging Centre
6875 Boulevard LaSalle
Montréal, QC H4H 1R3
gabriel.devenyi@mcgill.ca

INTRODUCTION

Magnetic resonance imaging is uniquely capable of capturing brain anatomy in vivo in humans with ever-improving accuracy.[1] MRI-derived measures of brain morphometry have been demonstrated to be powerful biomarkers capturing differences and changes associated with plasticity,[2,3] aging and development,[4,5] and disease and disease progression.[6-8] Deformation-based morphometry (DBM) is a registration-based technique that uses local volume changes derived from nonlinear deformation fields as a means of detecting local morphological differences/changes.[9-11] DBM does not require prior segmentation or definition of regions of interest (ROI), allowing for the detection of morphological changes in brain regions beyond the common techniques of classifier-driven voxel-based morphometry and cortical thickness analysis.

This technique has been extraordinarily useful in studying rodent models and local volume differences[12-20] where a readily accessible toolbox is available.[21,22] In preclinical models, it has been shown that the volume changes detected by DBM are associated with cellular modifications, such as changing synaptic density across brain networks.[23] While DBM can be used to compare subjects or groups of subjects cross-sectionally, it is particularly powerful when multiple measures of the same subject are available to model intra-individual time-dependent changes in vivo.[24] In humans, DBM has been shown to be sensitive and reliable in detecting local disease progression,[6,25,26] learning-induced plastic brain changes associated with musical training,[27] and individual brain changes following neuromodulatory treatments.[28,29]

Classically, DBM uses registration to a common template space (e.g. MNI152[30]) to derive the necessary deformation fields.[9,10] Previous work has shown that registration bias and risk of registration error are larger the greater the differences between the template and the individual brain.[31-33] These are especially relevant in the case of longitudinal studies, where the focus is on changes that occur within each individual brain. To capture these longitudinal individual changes, the deformation fields are best computed using within-subject registration, as even the use of a group-specific template would introduce bias and registration error. The superiority of the general principle of this technique was demonstrated by earlier work by Scahill and colleagues[34] who used serial fluid nonlinear registration to capture longitudinal within-subject changes in patients with presymptomatic, mild and moderate Alzheimer's disease.

Here we present a publicly available[35] two-level DBM pipeline using state-of-the-art registration tools[36,37] designed to capture within-subject changes accurately and allow for the comparison of individual morphological changes across subjects or groups. This two-level DBM technique first calculates the Jacobian determinants for each individual input MRI at the subject level using unbiased subject-specific templates and within-subject deformation fields; then, in a second step, the Jacobian determinants are transformed to an unbiased population common space to be used for statistical analysis. Using artificially induced volume changes and longitudinal images from the OASIS-2 dataset,[38] we demonstrate the superior sensitivity and accuracy of the two-level DBM pipeline and its lower probability of false positive results when studying longitudinal changes.

METHODS

IMPLEMENTATION

The two-level DBM pipeline is implemented as a Python wrapper around antsMultivariateTemplateConstruction2.sh[39] from the Advanced Normalization Tools (ANTs/2.5.0).[40] In the basic implementation, template construction is applied at two levels: the first level (typically within subject) is computed, generating an unbiased subject model and encoding the volumetric differences between input images in a deformation field relative to the subject-specific template (Figure 1). The first-level average templates are then fed into a second-level model build, which constructs an average representation of the population. Two types of Jacobian determinants are then computed at the first level: an absolute Jacobian, encoding voxel-wise, the nonlinear deformation field, combined with the affine determinant, and a relative Jacobian, where residual affine components present in the nonlinear deformation field are removed. The Jacobian maps are then resampled into the final common space and smoothed with a Gaussian kernel with a full-width-half-maximum of twice the smallest voxel size. An optional feature allows the unbiased average to be registered to a common space, such as an MNI model. The Jacobians can then be resampled into that space without contaminating estimated volume differences.

VALIDATION

RECOVERY OF ARTIFICIALLY INDUCED VOLUME DIFFERENCES

In order to test the sensitivity of this pipeline to volumetric differences in both one-level (i.e., cross-sectional, registration to one common template) and two-level (i.e., longitudinal, within-subject calculation of Jacobian determinants, followed by transformation to common space) implementations, we induced known volumetric changes in the left habenula and right anterior caudate in a set of T1w MRI scans and then used the various DBM pipelines to detect and recover those changes. We chose to use identical images with synthetic alterations in order to estimate the performance in an (artificial) best-case scenario, enabling an analysis of the upper bound of achieved sensitivity.

20 randomly selected T1w (11 female, age: 61-89 years, mean: 75.45 years ±7.95; 9 male, age: 66-84 years, mean: 72.44 years ±5.63) scans from the OASIS-2 dataset were preprocessed (minc-bpipe-library)[41] and affinely registered to MNI space. The left habenula and right anterior caudate were then semi-automatically segmented using MAGeTbrain.[42] These two structures were chosen as previous work demonstrated that region characteristics such as size have

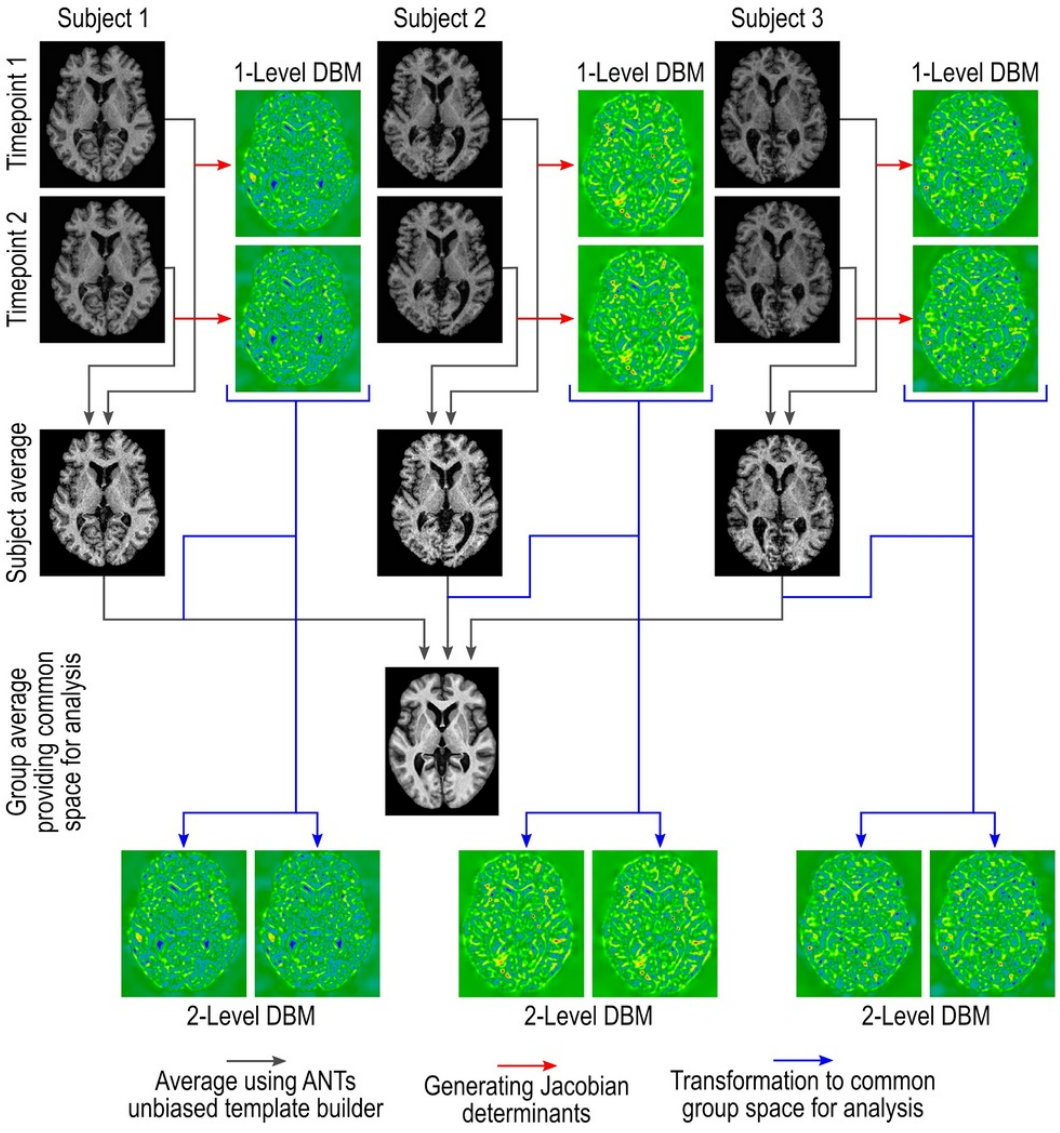

Figure 1. Illustration of the processing underlying the two-level DBM pipeline proposed.

Jacobian determinants for each individual input MRI are calculated at the subject level to capture differences and changes with maximal accuracy. The subject-level average brain is then used to generate an unbiased common space, and the Jacobians are transformed into that space for statistical analysis.

a small influence on registration sensitivity.[43] The labels were then used to generate deformation fields for specified Jacobian determinants of 0.5%, 1%, 2.11%, 4.47%, 9.45% and 20% (log spaced 0.5% to 20%) using disptools.[44] The resulting deformation fields were applied to a random subset of 10 of the subjects to produce a pseudo-second timepoint with an enlarged right habenula and reduced left anterior caudate volume of 0.5%, 1%, 2.11%, 4.47%, 9.45% and 20% (see supplementary video for an example of a modified caudate at 20%). The other 10 subjects were duplicated unchanged. The resulting datasets were constructed as a longitudinal study, with the original brains being used as the first time point, and the 10 modified brains used as the second time point while keeping the remaining 10 unchanged for the second time point (Figure 2). The resulting 6 (levels of local volume change) datasets were processed through the pipeline as both two-level (longitudinal within-subject registration to calculate Jacobian determinant, transformed to the unbiased average space for statistical comparison) and one-level (cross-sectional registration with Jacobian determinants generated relative to the unbiased group average).

Voxel-wise statistical modelling was performed using R/3.4.4 and RMINC/1.5.2.2 using mixed-effect linear models, with a fixed effect of (pseudo) timepoint and a random intercept by subject. Results were corrected for multiple comparisons using False Discovery Rate (FDR).[45] In addition to voxel-wise modelling, the individual segmentations were resampled into the final template space and merged via majority vote to produce masks. These masks were then used to calculate the volume of the target region by integration of the Jacobian values within the mask to be compared to the true segmentation volumes, thus allowing for an estimation of the effective volume difference captured by each of the pipeline implementations.

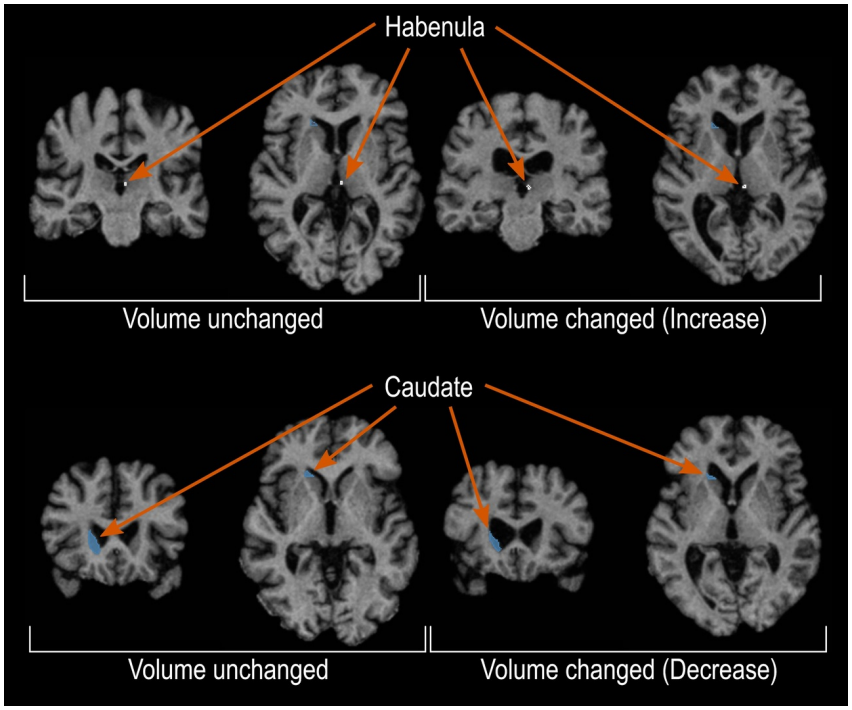

Figure 2. Two sets of brains, 10 brains that remained unchanged and a second set of 10 brains with synthetically induced volume changes to the habenula and caudate regions, were used to assess the sensitivity and accuracy of the two-level DBM.

The upper row shows an example of the increased volume in the right habenula region, and the lower row shows the decreased volume in the right caudate region.

EXPLORATORY ANALYSIS OF SAME DAY TEST-RETEST DATASET AND COMPARISON OF DBM IMPLEMENTATIONS

In order to explore the robustness of the pipeline to the intrinsic variations of repeated acquisitions, we obtained 15 subjects (15 randomly selected with two same day T1w images; 9 female, age: 19.6-55.6 years, mean: 33.0 years ±11.7; 6 male, age: 19.6-37.3 years, mean: 27.8 years ±6.5) from the Welsh Advanced Neuroimaging Database (WAND, [https://doi.gin.g-node.org/10.12751/g-node.5mv3bf/). Images were pre-processed using minc-bpipe-library (https://github.com/cobralab/minc-bpipe-library), and processed through 3 variants of the pipeline:

1. The recommended two-level longitudinal pipeline is rigidly initialized with the skull-stripped MNI model and upsampled to 0.5 mm isotropic (mni_icbm152_nlin_sym_09c). In this two-level pipeline, the Jacobian determinants for each individual input MRI are first calculated at the subject level using the within-subject deformation field. In a second step, these Jacobian determinants are then co-registered to an unbiased common space for statistical analysis.
2. The one-level pipeline with the same initialization. Here, the unbiased group average is used as the registration target, and the Jacobian determinants are calculated from the deformation field encompassing the full registration from the subject to the unbiased group average.
3. A modified version of the one-level pipeline to simulate classical DBM, where the previously mentioned model (MNI model upsampled to 0.5 mm isotropic) was used as the full-registration target, and only a single registration was completed.

The third variant aimed at comparing the results to more 'traditional' DBM pipelines that use a common brain template while maintaining the same registration tools.[9,10] The 2-level (longitudinal) and one-level (cross-sectional) final averages were post-registered to the MNI152 ICBM09c sym template using antsRegistrationSyN.sh (ANTS/2.5.0), and transformations were applied to statistical results so that final statistical maps could be compared head-to-head.

ANALYSIS OF AN ALZHEIMER'S DISEASE DATASET COMPARING DBM IMPLEMENTATIONS

In order to explore the sensitivity of the pipeline in capturing effects in a real dataset, we obtained the OASIS-2 dataset, which contains 150 subjects with 2-5 imaging sessions (mean 2.49, SD 0.69) for a total of 372 longitudinal T1w scans. The dataset consisted of 72 elderly healthy controls (HC; 50 female, Age: 75.5 ± 8.2), 64 participants with dementia (28 female, Age: 75.1 ± 6.7), and 14 patients (10 female, Age: 77.1 ± 7.7) who transitioned during the study between clinical classifications (i.e. from healthy to a diagnosis of dementia). Individuals underwent neurocognitive evaluation at each time point, including the Mini-Mental State Examination (MMSE). The T1W images were pre-processed using minc-bpipe-library (https://github.com/

cobralab/minc-bpipe-library), and the skull-stripped brains were processed through 3 variants of the pipeline as described above.

The 2-level (longitudinal) and one-level (cross-sectional) final averages were post-registered to the MNI152 ICBM09c sym template using antsRegistrationSyN.sh (ANTS/2.5.0), and transformations were applied to statistical results so that final statistical maps could be compared head-to-head; however, analysis was performed in the unbiased space in each case. Voxel-wise statistical modelling was performed using R/3.4.4 and RMINC/1.5.2.2 using mixed-effect linear models. The model tested the interaction effect of MMSE and days since first scan (as a proxy for disease progression), covaried for sex and age at first scan.

RESULTS

RECOVERY OF ARTIFICIALLY INDUCED VOLUME DIFFERENCES

Voxel-wise whole-brain mixed-effect models of the artificially induced volume changes are highly sensitive. Statistically significant effects are detected at FDR 5% threshold starting at the artificially induced 2% volume difference. Figure 3A shows a voxel-wise t-statistics map thresholded at 5% FDR. The one-level DBM statistical analysis does not reach statistically significant effects at FDR 5% until the 9% induced volume difference but only detects the caudate difference, not the habenula. Thus, from a voxel-wise analysis perspective, the two-level DBM detects volumetric differences that are ~4.5x smaller compared to a cross-sectional DBM model.

In addition to examining results on a voxel-wise statistical level, we also examine the inferred volumes estimated through the integration of the absolute Jacobians generated from the DBM within a consensus label. We can examine the resulting volumes with regard to how well they recover the volume difference between the original and induced-volume difference scans. Figure 3B shows the volume change captured by the DBM vs the induced volume difference for the habenula and caudate. The average values are reported in Table 1 showing that the two-level DBM captures the magnitude of the induced change with greater fidelity. Longitudinal volume effect sizes are recovered at approximately 50% of true volume as estimated by the integration of absolute Jacobians within a majority vote mask. Unmodified subjects in longitudinal DBM result in very small volume differences, as expected, whereas in one-level DBM, individual subjects can have volumetric error difference estimates of up to 5%.

To examine the possibility of bias in the DBM-based volume estimation, we generated plots illustrating estimated volume change and variance across all subjects (Supplementary Figure 1), which show the difference between true and estimated volumes compared to the true structure volume. The range of estimated volumes is substantially larger in the one-level models than the longitudinal models due to scan-wise volume estimates now being contaminated with deformations intended to create the final unbiased average, this is also an excellent visualization of the potential origin of method-related spurious results in the one-level model.

Considering that the only volumetric differences which exist between the subject-wise scans are known a priori, and the within-subject mixed-effect models, we can examine the potential findings incurred due to errors and biases related to methodological differences. The two 'timepoints' are composed of identical images except for the changes to the caudate and habenula regions, and we expect no findings beyond that. Computing a main effect of timepoint, we do find sizable groups of significant voxels showing effects using the one-level model ($p<0.01$, uncorrected). The two-level model, on the other hand, shows very few spurious voxels ($p<0.01$, uncorrected) (Figure 4). These spurious findings are most likely due to registration errors at the group average stage. As the Jacobian determinants for the two-level model are derived at the first within-subject stage, these errors likely have a much smaller effect on the final statistical comparison.

EXPLORATORY ANALYSIS OF SAME DAY TEST-RETEST DATASET AND COMPARISON OF DBM IMPLEMENTATIONS

DBM modelling of immediate (same day) test-retest T1w images demonstrates that the two-level DBM pipeline is robust and sensitivity, and less prone to produce potentially erroneous results as compared to the other implementations (Figure 5). This shows that results obtained using the two-level DBM pipeline likely more reliable.

ANALYSIS OF AN ALZHEIMER'S DISEASE DATASET COMPARING DBM IMPLEMENTATIONS

DBM modelling of the OASIS-2 dataset under the optimized longitudinal configuration reveals a global pattern of relative volume changes associated with a decrease in the MMSE score of participants. Firstly, increases in ventricular volume and CSF space adjacent to the temporal lobes were found, indicating an overall reduction in the volume of brain tissue. Secondly, a pattern of gray matter volume reduction in the temporal, frontal and parietal cortices. These effects are highly significant, surviving 1% FDR correction. When comparing the cross-sectional results of the same data, substantially fewer regions of frontal and parietal effects are present at the same threshold, indicating a reduction in sensitivity. Most concerningly, new effects showing an increase in volume of the right superior parietal cortex with increasing MMSE, indicating contamination of the longitudinal brain changes by a group-wise difference present at the start of the study, these effects are method-related spurious findings, as within-subject effects do not show these findings. Figure 6 shows the head-to-head comparison of the change in MMSE by time interaction in each of the respective unbiased spaces.

To benchmark the sensitivity of the unbiased DBM methods against classical methods, we also derived the Jacobian determinant performing a one-level DBM pipeline direct to MNI space similar to classical DBM methods.[9,10]

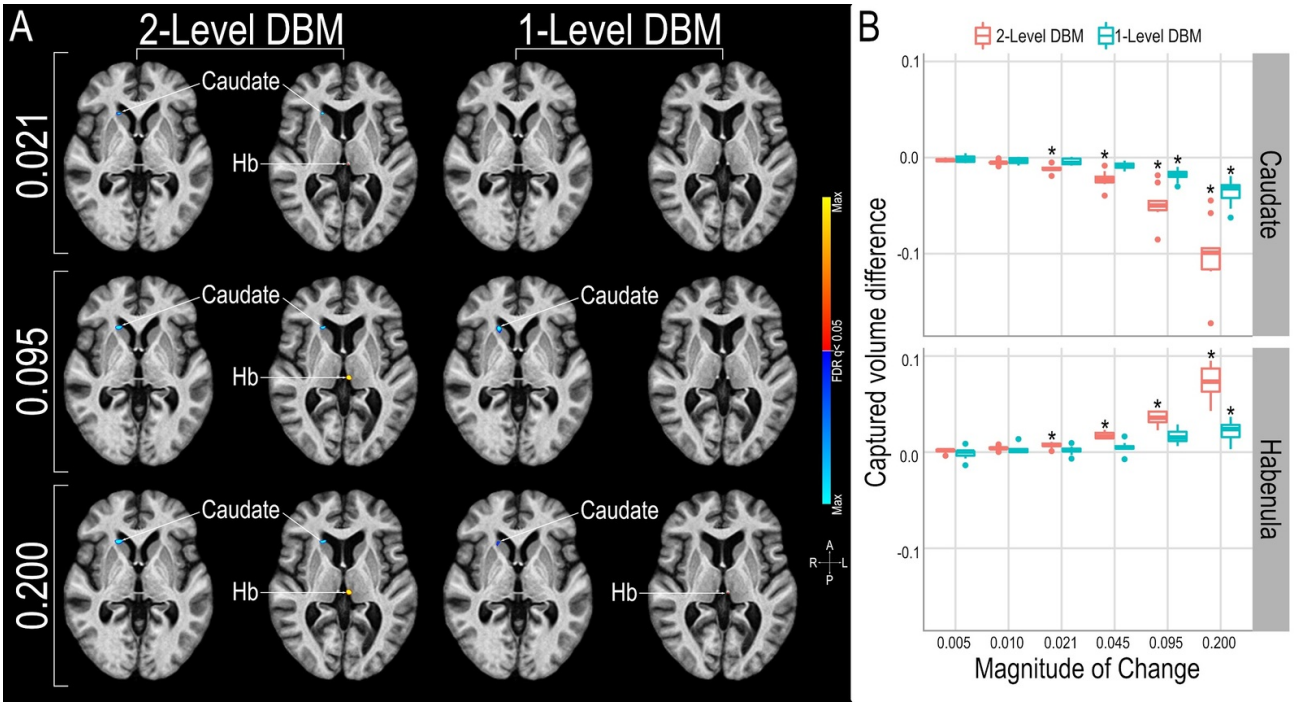

Figure 3. Results of the statistical analysis quantifying demonstrating the superior ability of the two-level DBM to detect and capture the magnitude of the induced volume change.

A) Axial section showing significant (FDR q<0.05) voxel-wise changes. The two-level DBM detects changed volumes at the habenula and caudate regions reliably from a magnitude of 0.021 onwards, while the one-level DBM only detects the induced change at the larger caudate region at 0.095 magnitudes of induced change. The one-level DBM only captures the volume change at the habenula region at an induced change of 0.2 magnitudes (20% increased voxel volume). B) Two-level DBM is superior to one level in capturing the magnitude of the induced change at about 50% level.

The classical DBM using MNI space instead of an unbiased group average shows a pattern of results that is very similar to the unbiased one-level DBM, including many of the same method-related spurious effects (Supplementary Figure 2). However, the sensitivity seems to be much reduced compared to the unbiased one-level DBM, as the sizes of groups of significant voxels are markedly reduced.

DISCUSSION

The collection of longitudinal data is fast becoming common in both public and private datasets, as well as preclinical, clinical, and population studies. Handling this data in an optimized two-level longitudinal way can yield higher power for a study than using one-level cross-sectional methods. In this study, we introduced a new deformation-based morphometry pipeline which implemented a multi-level unbiased template approach to measuring within-subject whole-brain volumetric change. We validated and compared it against other methods with both synthetic data and a real-world dataset. DBM, as opposed to voxel-based morphometry (VBM) pipelines, is usable without any tissue classification or atlas priors, allowing for arbitrary contrasts and application to novel species or anatomy. In addition, the absence of a classification stage means that datasets in which successful tissue classification cannot be performed are still usable for DBM. Finally, there are increasing concerns that the classical VBM implementations result in statistical bias due to circularity in their implementations.[46, 47] These prior-free implementations do not rely on such assumptions.

Validation of this pipeline using synthetic data reveals a supremely sensitive tool, approximately 4.5x more sensitive than cross-sectional modelling in detecting volumetric within-subject changes in group-wise comparisons. This result is obtained despite the variability in exact synthetic changes induced by the original manual segmentation process involved in defining the ROI for induced volume change. Very little work has been done in the area of synthetic DBM validation; only van Eede et. al[43] examined DBM in a rodent model. The two-level DBM implementation is able to capture roughly 50% of the intended change. It is most likely the case that the induced volume change did not reach the full level intended. This is due to resolution limitations, the resulting interpolation combined with the synthetic volume modification when creating an approximate deformation field. These factors will cause the final synthetic volume modification to be smaller than intended, making the fact that the two-level DBM implementation is able to capture roughly 50% of the intended change more remarkable.

It is also noteworthy that the induced volume changes are small. Given 1 mm isotropic MRI resolution, even a 20% voxel volume increase would not cause the outer boundary of a spherical structure, such as the structures used here, to change by a single voxel.

The two-level DBM not only demonstrates superior sensitivity in detecting longitudinal changes, it also demonstrates a diminished likelihood of providing method-related

Table 1. Volume change in either structure (caudate - volume decreased; habenula - volume increased) captured by one and two level DBM pipeline

Image type	Brain structure	Magnitude of induced change (in %)	Two-Level analysis volume change captured (in %)	One-Level analysis volume change captured (in %)
Volume Changed	caudate	-0.5	-0.28	-0.16
Volume Changed	caudate	-1.0	-0.50	-0.33
Volume Changed	caudate	-2.1	-1.12	-0.45
Volume Changed	caudate	-4.5	-2.29	-0.83
Volume Changed	caudate	-9.5	-4.85	-1.84
Volume Changed	caudate	-20.0	-10.14	-3.59
Volume Changed	habenula	+0.5	+0.13	-0.13
Volume Changed	habenula	+1.0	+0.42	+0.26
Volume Changed	habenula	+2.1	+0.69	+0.20
Volume Changed	habenula	+4.5	+1.74	+0.50
Volume Changed	habenula	+9.5	+3.58	+1.63
Volume Changed	habenula	+20.0	+7.37	+2.12
Volume Unchanged	caudate	0.0 (control for -0.5)	+0.01	+0.04
Volume Unchanged	caudate	0.0 (control for -1.0)	+0.02	+0.07
Volume Unchanged	caudate	0.0 (control for -2.1)	-0.05	+0.17
Volume Unchanged	caudate	0.0 (control for -4.5)	+0.01	-0.34
Volume Unchanged	caudate	0.0 (control for -9.5)	+0.04	-0.01
Volume Unchanged	caudate	0.0 (control for -20.0)	+0.01	-0.39
Volume Unchanged	habenula	0.0 (control for +0.5)	-0.02	+0.06
Volume Unchanged	habenula	0.0 (control for +1.0)	+0.06	+0.14
Volume Unchanged	habenula	0.0 (control for +2.1)	-0.05	-0.12
Volume Unchanged	habenula	0.0 (control for +4.5)	+0.03	-0.24
Volume Unchanged	habenula	0.0 (control for +9.5)	+0.06	+0.13
Volume Unchanged	habenula	0.0 (control for +20.0)	-0.01	-0.51

spurious positive results. Deriving the Jacobians from within-subject registration allows the minimization of registration bias. Bias grows when using different brain templates for registration, an unbiased group average or the MNI template.[31-33] This is apparent in the results when examining the much-expanded variance in the volume estimation in one version two-level DBM (Supplementary Figure 1), the method-related spurious positive findings (Figure 4 & Figure 5) and the differences in the pattern of significant voxels in the analysis of the OASIS-2 data (Figure 6, Supplementary Figure 2). These are likely caused by

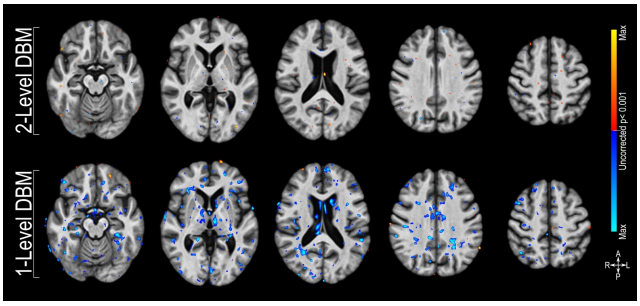

Figure 4. Statistical analysis using Jacobians derived using two-level DBM is less likely to produce method-related spurious findings.

Voxel-wise t-statistical maps (p<0.01) of the main effect of time computed using Jacobians derived from the two-level DBM (upper row) and one-level DBM (lower row). Except for the induced volume change to the caudate and habenula region in 10 of the 20 brains, identical brains were used for both 'timepoints', no effect of time should be found in this data.

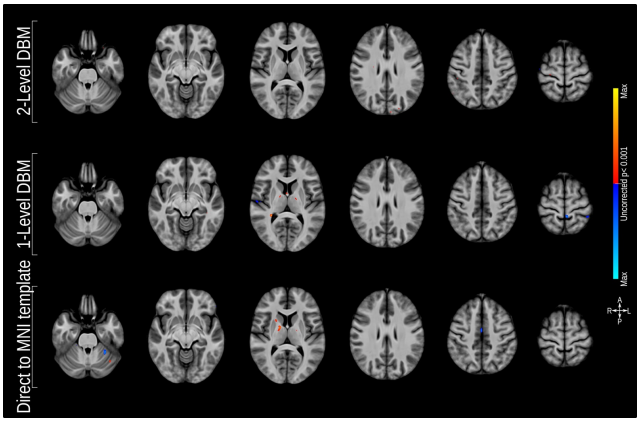

Figure 5. Axial sections showing uncorrected (p<0.001) apparent voxel-wise volume changes in 15 subjects scanned repeatedly (on the same day) captured using the Jacobians derived using two-level DBM, one-level, and one-level DBM to template space (the "classical" DBM method).

registration errors. The two-level DBM reduces this leading to more reliable findings.

The two-level DBM pipeline reported here has already been applied successfully, detecting changes in patients following neuromodulatory treatment for refractory aggressive behaviour[28] or mood disorder,[29] identifying differences in patients with schizophrenic behaviour,[48] and aiding the localization of physiological effects of drug treatments in psychosis.[49] It has been applied to show how cerebellar and subcortical atrophy contribute to psychiatric symptoms in frontotemporal dementia.[50] It has also been adapted to investigate brain morphology differences and changes in preclinical models.[51,52]

CONCLUSION

Here, we present a two-level DBM technique, where the Jacobian determinants are first calculated at the subject level

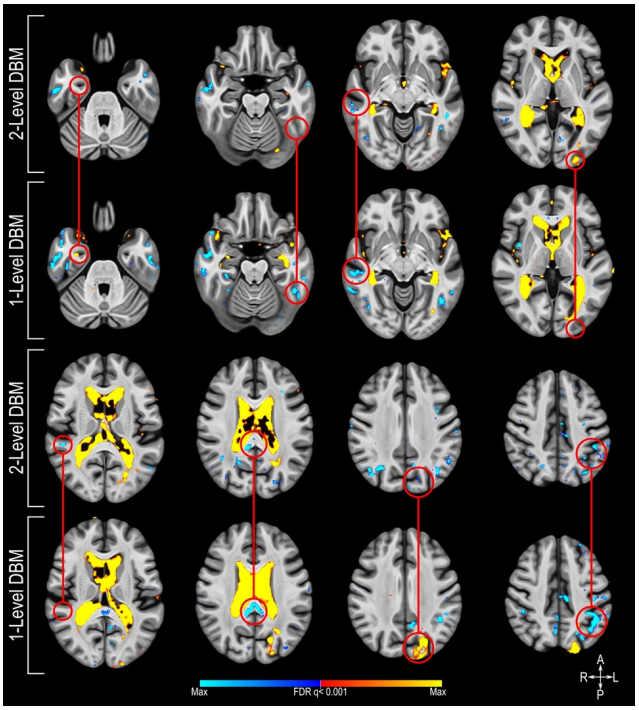

Figure 6. Axial sections showing significant (FDR q<0.01) voxel-wise volume changes captured using the Jacobians derived using one and two-level DBM associated with increasing MMSE score over time.

Red circles highlight areas where the one-level DBM fails to capture a difference or where it produces spurious results.

followed by co-registration to an unbiased common group average. This two-level DBM is particularly suitable for capturing longitudinal intra-individual changes in vivo, being 4.5x more sensitive in detecting longitudinal within-subject volume changes compared to a typical one-level DBM approach and capturing the magnitude of the change much more accurately. The pipeline is publicly available[35,53] and will provide users with a superior alternative to analyze brain morphology, especially when using longitudinal data.

DATA AND CODE AVAILABILITY

This study utilizes open-access data. The code used for data processing and analysis is publicly available at GitHub: https://github.com/CoBrALab/twolevel_ants_dbm & https://github.com/CoBrALab/optimized_antsMultivariateTemplateConstruction (accessed March 19, 2025)

ACKNOWLEDGEMENTS

Computations were performed on the Niagara supercomputer at the SciNet HPC Consortium. SciNet is funded by Innovation, Science and Economic Development Canada; the Digital Research Alliance of Canada; the Ontario Research Fund: Research Excellence; and the University of Toronto.

FUNDING SOURCES

The authors received no financial support for the research, authorship, or publication of this article.

CONFLICTS OF INTEREST

The authors declare that they have no conflicts of interest related to this work.

Submitted: August 09, 2024 CDT. Accepted: March 18, 2025 CDT. Published: April 14, 2025 CDT.

REFERENCES

1. Lerch JP, van der Kouwe AJW, Raznahan A, Paus T, Johansen-Berg H, Miller KL, et al. Studying neuroanatomy using MRI. *Nat Neurosci*. 2017;20(3):314-326. doi:10.1038/nn.4501

2. Maguire EA, Gadian DG, Johnsrude IS, Good CD, Ashburner J, Frackowiak RS, et al. Navigation-related structural change in the hippocampi of taxi drivers. *Proc Natl Acad Sci U S A*. 2000;97(8):4398-4403. doi:10.1073/pnas.070039597

3. Hyde KL, Zatorre RJ, Griffiths TD, Lerch JP, Peretz I. Morphometry of the amusic brain: a two-site study. *Brain*. 2006;129(Pt 10):2562-2570. doi:10.1093/brain/awl204

4. Bedford SA, Park MTM, Devenyi GA, Tullo S, Germann J, Patel R, et al. Large-scale analyses of the relationship between sex, age and intelligence quotient heterogeneity and cortical morphometry in autism spectrum disorder. *Mol Psychiatry*. 2020;25(3):614-628. doi:10.1038/s41380-019-0420-6

5. Lei D, Qin K, Li W, Pinaya WHL, Tallman MJ, Rodrigo Patino L, et al. Brain morphometric features predict medication response in youth with bipolar disorder: a prospective randomized clinical trial. *Psychol Med*. Published online 2023:1-11. doi:10.1017/S0033291722000757

6. Manera AL, Dadar M, Collins DL, Ducharme S, Frontotemporal Lobar Degeneration Neuroimaging Initiative. Deformation based morphometry study of longitudinal MRI changes in behavioral variant frontotemporal dementia. *Neuroimage Clin*. 2019;24:102079. doi:10.1016/j.nicl.2019.102079

7. Zeighami Y, Ulla M, Iturria-Medina Y, Dadar M, Zhang Y, Larcher KMH, et al. Network structure of brain atrophy in de novo Parkinson's disease. *Elife*. 2015;4:4. doi:10.7554/eLife.08440

8. McCarthy J, Collins DL, Ducharme S. Morphometric MRI as a diagnostic biomarker of frontotemporal dementia: A systematic review to determine clinical applicability. *Neuroimage Clin*. 2018;20:685-696. doi:10.1016/j.nicl.2018.08.028

9. Ashburner J, Hutton C, Frackowiak R, Johnsrude I, Price C, Friston K. Identifying Global Anatomical Differences: Deformation-Based Morphometry. *Human Brain Mapping*. 1998;6:348-357. doi:10.1002/(SICI)1097-0193(1998)6:5/6

10. Chung MK, Worsley KJ, Paus T, Cherif C, Collins DL, Giedd JN, et al. A unified statistical approach to deformation-based morphometry. *Neuroimage*. 2001;14:595-606. doi:10.1006/nimg.2001.0862

11. Davatzikos C. Spatial transformation and registration of brain images using elastically deformable models. *Comput Vis Image Underst*. 1997;66(2):207-222. doi:10.1006/cviu.1997.0605

12. Scholz J, Niibori Y, W Frankland P, P Lerch J. Rotarod training in mice is associated with changes in brain structure observable with multimodal MRI. *Neuroimage*. 2015;107:182-189. doi:10.1016/j.neuroimage.2014.12.003

13. Jung H, Park H, Choi Y, Kang H, Lee E, Kweon H, et al. Sexually dimorphic behavior, neuronal activity, and gene expression in Chd8-mutant mice. *Nat Neurosci*. Published online 2018. doi:10.1038/s41593-018-0208-z

14. Scholz J, Allemang-Grand R, Dazai J, Lerch JP. Environmental enrichment is associated with rapid volumetric brain changes in adult mice. *Neuroimage*. 2015;109:190-198. doi:10.1016/j.neuroimage.2015.01.027

15. Ellegood J, Anagnostou E, Babineau BA, Crawley JN, Lin L, Genestine M, et al. Clustering autism: using neuroanatomical differences in 26 mouse models to gain insight into the heterogeneity. *Mol Psychiatry*. 2015;20(1):118-125. doi:10.1038/mp.2014.98

16. Szulc KU, Lerch JP, Nieman BJ, Bartelle BB, Friedel M, Suero-Abreu GA, et al. 4D MEMRI atlas of neonatal FVB/N mouse brain development. *Neuroimage*. 2015;118:49-62. doi:10.1016/j.neuroimage.2015.05.029

17. Avivi-Arber L, Seltzer Z 'ev, Friedel M, Lerch JP, Moayedi M, Davis KD, et al. Widespread Volumetric Brain Changes following Tooth Loss in Female Mice. *Front Neuroanat*. 2016;10:121. doi:10.3389/fnana.2016.00121

18. Qiu LR, Germann J, Spring S, Alm C, Vousden DA, Palmert MR, et al. Hippocampal volumes differ across the mouse estrous cycle, can change within 24 hours, and associate with cognitive strategies. *Neuroimage*. 2013;83:593-598. doi:10.1016/j.neuroimage.2013.06.074

19. Lerch JP, Yiu AP, Martinez-Canabal A, Pekar T, Bohbot VD, Frankland PW, et al. Maze training in mice induces MRI-detectable brain shape changes specific to the type of learning. *Neuroimage*. 2011;54(3):2086-2095. doi:10.1016/j.neuroimage.2010.09.086

20. Cahill LS, Steadman PE, Jones CE, Laliberté CL, Dazai J, Lerch JP, et al. MRI-detectable changes in mouse brain structure induced by voluntary exercise. *Neuroimage*. 2015;113:175-183. doi:10.1016/j.neuroimage.2015.03.036

21. Website. https://wiki.mouseimaging.ca/display/MICePub/Pydpiper

22. Friedel M, van Eede MC, Pipitone J, Chakravarty MM, Lerch JP. Pydpiper: a flexible toolkit for constructing novel registration pipelines. *Front Neuroinform*. 2014;8:67. doi:10.3389/fninf.2014.00067

23. Chakravarty MM, Hamani C, Martinez-Canabal A, Ellegood J, Laliberté C, Nobrega JN, et al. Deep brain stimulation of the ventromedial prefrontal cortex causes reorganization of neuronal processes and vasculature. *Neuroimage*. 2016;125:422-427. doi:10.1016/j.neuroimage.2015.10.049

24. Lerch JP, Gazdzinski L, Germann J, Sled JG, Henkelman RM, Nieman BJ. Wanted dead or alive? The tradeoff between in-vivo versus ex-vivo MR brain imaging in the mouse. *Front Neuroinform*. 2012;6:6. doi:10.3389/fninf.2012.00006

25. Janke AL, De Zubicaray G, Rose SE, Griffin M, Chalk JB, Galloway GJ. 4D deformation modeling of cortical disease progression in Alzheimer's dementia. *Magn Reson Med*. 2001;46(4):661-666. doi:10.1002/mrm.1243

26. Tessa C, Lucetti C, Giannelli M, Diciotti S, Poletti M, Danti S, et al. Progression of brain atrophy in the early stages of Parkinson's disease: a longitudinal tensor-based morphometry study in de novo patients without cognitive impairment. *Hum Brain Mapp*. 2014;35(8):3932-3944. doi:10.1002/hbm.22449

27. Hyde KL, Lerch J, Norton A, Forgeard M, Winner E, Evans AC, et al. Musical training shapes structural brain development. *J Neurosci*. 2009;29(10):3019-3025. doi:10.1523/JNEUROSCI.5118-08.2009

28. Gouveia FV, Germann J, de Morais R, Fonoff ET, Hamani C, Alho EJ, et al. Longitudinal Changes After Amygdala Surgery for Intractable Aggressive Behavior: Clinical, Imaging Genetics, and Deformation-Based Morphometry Study-A Case Series. *Neurosurgery*. 2021;88(2):E158-E169. doi:10.1093/neuros/nyaa378

29. Elias GJB, Germann J, Boutet A, Pancholi A, Beyn ME, Bhatia K, et al. Structuro-functional surrogates of response to subcallosal cingulate deep brain stimulation for depression. *Brain*. Published online July 29, 2021. doi:10.1093/brain/awab284

30. Fonov VS, Evans AC, McKinstry RC, Almli CR, Collins DL. Unbiased nonlinear average age-appropriate brain templates from birth to adulthood. *Neuroimage*. 2009;47:S102. doi:10.1016/S1053-8119(09)70884-5

31. Fonov V, Evans AC, Botteron K, Almli CR, McKinstry RC, Collins DL, et al. Unbiased average age-appropriate atlases for pediatric studies. *Neuroimage*. 2011;54(1):313-327. doi:10.1016/j.neuroimage.2010.07.033

32. Yoon U, Fonov VS, Perusse D, Evans AC, Brain Development Cooperative Group. The effect of template choice on morphometric analysis of pediatric brain data. *Neuroimage*. 2009;45(3):769-777. doi:10.1016/j.neuroimage.2008.12.046

33. Wu Y, Ridwan AR, Niaz MR, Alzheimer's Disease Neuroimaging Initiative, Bennett DA, Arfanakis K. High resolution 0.5mm isotropic T1-weighted and diffusion tensor templates of the brain of non-demented older adults in a common space for the MIITRA atlas. *Neuroimage*. 2023;282:120387. doi:10.1016/j.neuroimage.2023.120387

34. Scahill RI, Schott JM, Stevens JM, Rossor MN, Fox NC. Mapping the evolution of regional atrophy in Alzheimer's disease: unbiased analysis of fluid-registered serial MRI. *Proc Natl Acad Sci U S A*. 2002;99(7):4703-4707. doi:10.1073/pnas.052587399

35. GitHub - CoBrALab/optimized_antsMultivariateTemplateConstruction: A re-implementation of antsMultivariateTemplateConstruction2.sh using optimized image pyramid scale-space and qbatch support. GitHub. Accessed July 29, 2024. https://github.com/CoBrALab/optimized_antsMultivariateTemplateConstruction

36. Avants BB, Tustison NJ, Song G, Cook PA, Klein A, Gee JC. A reproducible evaluation of ANTs similarity metric performance in brain image registration. *Neuroimage*. 2011;54(3):2033-2044. doi:10.1016/j.neuroimage.2010.09.025

37. Klein A, Andersson J, Ardekani BA, Ashburner J, Avants B, Chiang MC, et al. Evaluation of 14 nonlinear deformation algorithms applied to human brain MRI registration. *Neuroimage*. 2009;46(3):786-802. doi:10.1016/j.neuroimage.2008.12.037

38. Marcus DS, Fotenos AF, Csernansky JG, Morris JC, Buckner RL. Open Access Series of Imaging Studies (OASIS): Longitudinal MRI Data in Nondemented and Demented Older Adults. *J Cogn Neurosci*. 2010;22(12):2677-2684. doi:10.1162/jocn.2009.21407

39. ANTs/Scripts/antsMultivariateTemplateConstruction2.sh at master · ANTsX/ANTs. GitHub. Accessed July 29, 2024. https://github.com/ANTsX/ANTs/blob/master/Scripts/antsMultivariateTemplateConstruction2.sh

40. Website. http://stnava.github.io/ANTs/

41. GitHub - CoBrALab/minc-bpipe-library: Library of bpipe implemented commands commonly applied to minc datafiles, suitable for importing into other pipelines. GitHub. Accessed November 20, 2024. https://github.com/CoBrALab/minc-bpipe-library

42. Chakravarty MM, Steadman P, van Eede MC, Calcott RD, Gu V, Shaw P, et al. Performing label-fusion-based segmentation using multiple automatically generated templates. *Hum Brain Mapp*. 2013;34(10):2635-2654. doi:10.1002/hbm.22092

43. van Eede MC, Scholz J, Chakravarty MM, Henkelman RM, Lerch JP. Mapping registration sensitivity in MR mouse brain images. *Neuroimage*. 2013;82:226-236. doi:10.1016/j.neuroimage.2013.06.004

44. GitHub - m-pilia/disptools: Generate displacement fields with known volume changes. GitHub. Accessed July 30, 2024. https://github.com/m-pilia/disptools

45. Benjamini Y, Hochberg Y. Controlling the false discovery rate: A practical and powerful approach to multiple testing. *J R Stat Soc Series B Stat Methodol*. 1995;57(1):289-300. doi:10.1111/j.2517-6161.1995.tb02031.x

46. Tustison NJ, Avants BB, Cook PA, Gee JC, Stone JR. Statistical bias in optimized VBM. In: Weaver JB, Molthen RC, eds. *Medical Imaging 2013: Biomedical Applications in Molecular, Structural, and Functional Imaging*. Vol 8672. SPIE Proceedings. International Society for Optics and Photonics; 2013:86720U. doi:10.1117/12.2006377

47. Tustison NJ, Avants BB, Cook PA, Kim J, Whyte J, Gee JC, et al. Logical circularity in voxel-based analysis: normalization strategy may induce statistical bias. *Hum Brain Mapp*. 2014;35(3):745-759. doi:10.1002/hbm.22211

48. Kirschner M, Shafiei G, Markello RD, Makowski C, Talpalaru A, Hodzic-Santor B, et al. Latent Clinical-Anatomical Dimensions of Schizophrenia. *Schizophr Bull*. 2020;46(6):1426-1438. doi:10.1093/schbul/sbaa097

49. Livingston NR, Kiemes A, Devenyi GA, Knight S, Lukow PB, Jelen LA, et al. Effects of diazepam on hippocampal blood flow in people at clinical high risk for psychosis. *Neuropsychopharmacology*. 2024;49(9):1448-1458. doi:10.1038/s41386-024-01864-9

50. Bussy A, Levy JP, Best T, Patel R, Cupo L, Van Langenhove T, et al. Cerebellar and subcortical atrophy contribute to psychiatric symptoms in frontotemporal dementia. *Hum Brain Mapp*. 2023;44(7):2684-2700. doi:10.1002/hbm.26220

51. Guma E, Snook E, Spring S, Lerch JP, Nieman BJ, Devenyi GA, et al. Subtle alterations in neonatal neurodevelopment following early or late exposure to prenatal maternal immune activation in mice. *Neuroimage Clin*. 2021;32:102868. doi:10.1016/j.nicl.2021.102868

52. Nasseef MT, Devenyi GA, Mechling AE, Harsan LA, Chakravarty MM, Kieffer BL, et al. Deformation-based Morphometry MRI Reveals Brain Structural Modifications in Living Mu Opioid Receptor Knockout Mice. *Front Psychiatry*. 2018;9:411712. doi:10.3389/fpsyt.2018.00643

53. GitHub - CoBrALab/twolevel_ants_dbm: A twolevel deformation based morphometry pipeline using ants. GitHub. Accessed July 30, 2024. https://github.com/CoBrALab/twolevel_ants_dbm

SUPPLEMENTARY MATERIALS

Supplementary Material

Download: https://apertureneuro.org/article/133510-longitudinal-deformation-based-morphometry-pipeline-to-study-neuroanatomical-differences-in-structural-mri-based-on-syn-unbiased-templates/attachment/273611.pdf

Supplementary Video

Download: https://apertureneuro.org/article/133510-longitudinal-deformation-based-morphometry-pipeline-to-study-neuroanatomical-differences-in-structural-mri-based-on-syn-unbiased-templates/attachment/273612.mp4